Available online at www.sciencedirect.com
SCIENCE DIRECT®
Journal of Applied Geophysics 53 (2003) 103–120
JOURNAL OF APPLIED GEOPHYSICS
www.elsevier.com/locate/jappgeo

Removal of power-line harmonics from proton magnetic resonance measurements

Anatoly Legchenko[a,*], Pierre Valla[b]

[a] BRGM, BP 6009, 45060 Orléans Cedex, France
[b] IRIS-Instruments, BP 6007, 45060 Orléans Cedex, France

Received 15 March 2001; accepted 13 May 2003

Abstract

The Magnetic Resonance Sounding (MRS) method is based on the resonance behaviour of proton magnetic moments in the geomagnetic field. The main distinction between MRS and other geophysical methods is that it measures the magnetic resonance signal directly from groundwater molecules, making it a selective tool sensitive to groundwater. As the signal generated by the protons is very small, the method is also sensitive to electromagnetic interference (noise) and this is one of the major limitations for practical application. The frequency of the magnetic resonance signal (the Larmor frequency) is directly proportional to the magnitude of the geomagnetic field and varies between 800 and 2800 Hz around the globe. Whilst natural noise within this frequency range is generally not very large (excepting magnetic storms or other temporary disturbances), the level of cultural noise (electrical power lines, generators, etc.) may be very high. In order to improve performance, three existing filtering techniques were adapted to processing MRS measurements: block subtraction, sinusoid subtraction and notch filtering. The first two are subtraction techniques capable of suppressing stationary power-line noise without distorting or attenuating the signal of interest, both involve subtracting an estimate of the harmonic component but differ in the way the component is estimated. The block subtraction method consists of ascertaining the power-line noise (or ''noise block'') from a record of the noise alone, and then subtracting this block from a record containing both the noise and the signal. The sinusoid subtraction method is based on the calculation of the amplitude, frequency and phase of power-line harmonics using noise records. The notch filtering method does not require knowledge of the power-line harmonic parameters but it may cause distortion of the measured signal. During the study, it was found that, in the investigated frequency range, the electromagnetic noise produced by electrical power lines was much less stable and regular than expected. The proportion of 50 Hz harmonics (regular part) in the noise energy is site-dependent and may vary between 20% and 50%. Whilst the power-line harmonics are seen clearly on the noise spectra, the amplitude and frequency of each harmonic may vary significantly from one record to another. Under these conditions, any block subtraction scheme based on a high noise regularity cannot be used systematically. The sinusoid subtraction is generally more efficient than the block subtraction and its application allows noise reduction by a factor of up to nearly 5. The notch filtering technique was studied further using a synthetic signal mixed with real noise and the results show that the noise can be reduced by factors of 2–10. The efficiency of the investigated filtering techniques is site-dependent. Three important factors define how successfully noise can be filtered from the signal record: the difference between the Larmor frequency and the nearest power-line harmonic frequency; the relaxation time of the magnetic resonance signal; and the proportion of the regular part of the noise spectrum. In most cases though, the improvement achieved in the critical signal-to-

* Corresponding author.
E-mail address: Legtchenko@exchange.brgm.fr (A. Legchenko).

doi:10.1016/S0926-9851(03)00041-7

noise ratio (S/N) (5- to 8-fold on average) enables MRS application to be extended towards more noisy areas. The efficiency of the notch filtering technique applied to MRS measurements is demonstrated by a field example from France.

Keywords: Groundwater; MRS; Surface NMR; RMP; Power-line harmonics

1. Introduction

The Magnetic Resonance Sounding (MRS) method for groundwater investigation is based on the resonance behaviour of proton magnetic moments in the geomagnetic field (Semenov et al., 1989; Schirov et al., 1991). The main feature that distinguishes MRS from other geophysical methods is that it measures a magnetic resonance signal generated by groundwater molecules, and is therefore an excellent tool for groundwater detection. It has also been shown experimentally that, using an empirical relationship, MRS can enable estimates of aquifer permeability (Legchenko et al., 2002).

One of the major limitations of this technique is the sensitivity to natural and man-made noise. Indeed, an alternating magnetic field produced by the precession of proton magnetic moments in groundwater varies between 10^{-12} and 4×10^{-9} T. The voltage created by this magnetic field (MRS signal) varies between 10 and 4000 nV when using a wire loop of 100 m diameter as a receiving antenna, and contrary to many geophysical techniques, the signal cannot be amplified by increasing the transmitter power. The frequency of the magnetic resonance signal (the Larmor frequency) is directly proportional to the magnitude of the geomagnetic field and varies between 800 and 2800 Hz around the globe. Usually, MRS can be used without major problems within this frequency range because the natural noise is sufficiently low. However, in areas where industrial noise is much stronger than natural noise, power-line harmonics may create a major problem, particularly when the Larmor frequency is close to one of the harmonics of the fundamental frequency (50 or 60 Hz).

Harmonic noise generated by power lines can be detrimental not only for MRS but also for other geophysical methods, and this has stimulated several different approaches to noise reduction. For this study, the subtraction technique developed by Butler and Russell (1993) for processing seismo-electric measurements was selected. The technique is capable of suppressing stationary power-line noise without distorting or attenuating the signal of interest. It involves subtracting an estimate of the harmonic component, with two different ways of estimating the component. However, the approach assumes stability and regularity, for at least a few seconds, of industrial noise generated by sources such as power lines. It remains to be established whether the amplitude, phase and frequency of power-line harmonics within the selected frequency range are stable enough for a successful application of this scheme.

In order to complete the study, investigations were carried out on the efficiency of the well-known notch filtering technique applied to filtering of magnetic resonance records. This method is less sensitive to power-line harmonics instability but introduces some distortion, the extent of which, for magnetic resonance records, depends upon the relative shift between the Larmor frequency and the harmonics frequencies, and also upon the relaxation time of the signal.

As the MRS method is relatively new, some basic principles are described below.

2. Magnetic resonance sounding

2.1. Review of the basic principles

To an outside observer, MRS appears very similar to Transient EM when a coincident transmitting/receiving loop is used. A wire loop is laid out on the ground, normally in a circle with 10–200 m diameter depending on the depth of the target aquifer; it may also be laid out in a square or, to improve signal-to-noise ratio (S/N), in a "figure of eight" shape (Trushkin et al., 1994). The antenna is then energized by a pulse of alternating current

$$i(t) = I_0\cos(\omega_0 t),\ 0 < t \le \tau, \tag{1}$$

where I_0 and τ, respectively, are the pulse amplitude and duration. The frequency of the current $\omega_0 = 2\pi f_0$ is set equal to the Larmor frequency of the protons in the geomagnetic field $\omega_0 = \gamma B_0$, with B_0 being the magnitude of the geomagnetic field and γ the gyromagnetic ratio for protons (a physical constant). The Larmor frequency is usually known from measurements of the geomagnetic field B_0 using a proton magnetometer.

The pulse causes precession of the protons around the geomagnetic field, which creates an alternating magnetic field that can be detected using the same antenna after the pulse is terminated. However, in practise, the magnetic resonance response recording is possible only after an instrumental delay (''dead time''). Oscillating with the Larmor frequency, the signal $e(t,q)$ has an exponential envelope and depends on the pulse parameter $q = I_0\tau$:

$$e(t,q) = e_0(q)\exp(-t/T_2^*(q))\sin(\omega_0 t + \varphi_0(q)), \quad (2)$$

where $T_2^*(q)$ is the spin–spin relaxation time, and $\varphi_0(q)$ is the phase of the MRS signal.

The MRS signal is measured for different values of the pulse parameter q. Assuming that the stratification is horizontal and the vertical distribution of resistivity is known ($\rho(r) = \rho(z)$), the MRS imaging equation can be simplified to an integral equation (Legchenko and Valla, 2002)

$$e_0(t,q) = \int_V K(q,z)w(z)\exp(-t/T_2^*(z))\mathrm{d}z, \quad (3)$$

where $K(q,z)$ is the kernel, and $0 \le w(z) \le 1$ is the water content. The water content $w(z)$ indicates the presence of aquifers: $w \to 0$ corresponds to dry or compact rocks and $w \to 1$ to lake water. The relaxation time $T_2^*(z)$ correlates with the mean size of pores in water-saturated rock; it varies typically from 40 ms in very fine sand to 400 ms in gravel.

2.2. NUMIS records

The standard NUMIS (IRIS Instruments) MRS equipment acquires data in the form of time series recorded before and after the pulse transmission. Each record before the pulse is considered as noise only, whereas records after the pulse contain both signal and noise. Before digitizing, a hardware band-pass filter with a ± 100 Hz bandwidth (at the 3-dB level) centred at the excitation pulse frequency is applied. This central frequency is set to equal the Larmor frequency measured by proton magnetometer at each investigated site. The time diagram of the signal measurement process is shown in Fig. 1.

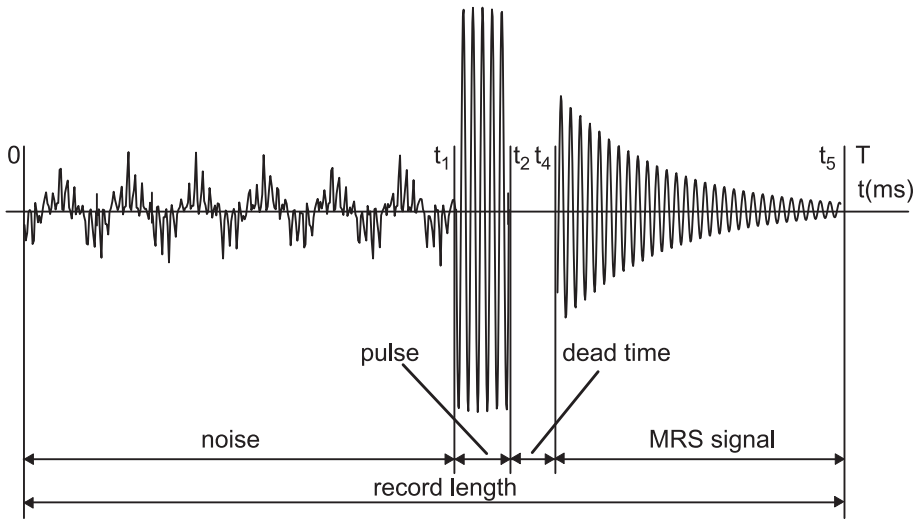

Fig. 1. NUMIS record.

For spectral analysis, the time series are digitized with a sampling frequency four times higher than the Larmor frequency ($f_s = 4f_0$) so as to fully satisfy Shannon's sampling theorem, and to allow full and accurate recovery of both noise and signal passing through the hardware filter. For measuring the signal envelope, a synchronous detector with a low-pass filter of 100 Hz band-pass (at the 3-dB level) is applied (Max, 1981). After the synchronous detection, the sampling frequency is set at 500 Hz.

The synchronous detector has two channels (X and Y). For both channels, the reference frequency (f_{sd}) is set as close as possible to the signal frequency, that is the Larmor frequency (f_0). The phase of the reference frequency for the X channel coincides with the phase of the current in the loop, and the phase of the frequency for the Y channel is shifted 90°. The amplitude and phase of the signal after the synchronous detector are $A(t) = \sqrt{X^2(t) + Y^2(t)}$ and $\Phi(t) = \tan^{-1}(Y(t)/X(t))$, respectively.

In this way, two derived signals are obtained, one in phase and one out of phase:

$$X(t) = e_0 \exp(-t/T_2^*)\cos(\delta\omega t + \varphi_0) + \sum_K p_k \cos(\delta\omega_k t + \varphi_k) + \varepsilon_X(t), \quad (4)$$

$$Y(t) = e_0 \exp(-t/T_2^*)\sin(\delta\omega t + \varphi_0) + \sum_K p_k \sin(\delta\omega_k t + \varphi_k) + \varepsilon_Y(t), \quad (5)$$

where $\delta\omega = 2\pi\delta f = 2\pi(f_{sd} - f_0)$; p_k, $\delta\omega_k = 2\pi\delta f_k = 2\pi(f_{sd} - f_k)$ and φ_k are the amplitude, the frequency and phase of the kth power-line harmonic (with K being the number of harmonics passed through the hardware filter); and $\varepsilon = \sqrt{\varepsilon_X^2 + \varepsilon_Y^2}$ is the nonregular noise.

For obtaining e_0 and T_2^* it is assumed that $e_0 \gg \varepsilon + \sum_K p_k$ and, thus, the logarithm of the measured amplitude can be calculated, followed by a linear regression fit:

$$\log(A) = \log(e_0) - t/T_2^* + \sum_K p_{Lk}(t) + \varepsilon_L(t), \quad (6)$$

where $\sum_K p_{Lk}(t)$ and $\varepsilon_L(t)$ is the logarithmic noise induced by the noise components X and Y. The phase of the measured signal at time t is composed of the initial phase φ_0 plus the phase shift caused by the frequency offset between the signal frequency and the synchronous detector reference frequency:

$$\Phi(t) = \delta\omega t + \varphi_0 + \varphi_p(t) + \varphi_\varepsilon(t), \quad (7)$$

where $\varphi_p(t) + \varphi_\varepsilon(t)$ is the phase instability caused by the regular and nonregular noise. A linear regression fit is then applied to determine $\delta\omega$ and hence f_0 and φ_0.

The linear regression fit provides a reliable estimate of signal parameters when the noise is low. However, the algorithm is sensitive to noise and, in order to diminish noise influence, a nonlinear regression curve-fitting technique based on least squares minimisation must be used:

$$\left[\int_{t_4}^{t_5} (X(t) - X_{mod}(t))^2 dt + \int_{t_4}^{t_5} (Y(t) - Y_{mod}(t))^2 dt\right] \rightarrow \min, \quad (8)$$

where $(t_5 - t_4)$ is the record length (Fig. 1), $X_{mod}(t) = e_0 \cos(\delta\omega t + \varphi_0)\exp(-t/T_2^*)$ and $Y_{mod}(t) = e_0 \sin(\delta\omega t + \varphi_0)\exp(-t/T_2^*)$. For minimisation, the Marquardt nonlinear fitting technique (Marquardt, 1963) was used, with the starting point derived from the linear regression estimate presented above (Legchenko and Valla, 1998).

3. Electromagnetic noise generated by electrical power lines

A special field study was undertaken in order to learn more about industrial noise. The frequency range of interest for the MRS method is between 800 and 2800 Hz, which corresponds to worldwide variations of the Larmor frequency set by the earth's magnetic field. The study was carried out mainly in areas with the Larmor frequency around 2000 Hz, but it is likely that this does not change the general nature of the results. The field data were recorded in France and also in other countries; field data in this paper were acquired at three sites in France, one in Israel, one in the Netherlands and one in the USA. Table 1 summarises the characteristics of data acquisition parameters at these test sites. A noise-reducing fig-

Table 1
Summary of investigated sites

Site	Record before the pulse (ms)	Record after the pulse (ms)	Industrial frequency (Hz)	Frequency range (Hz)	Central frequency (Hz)
France (Site 1)	1000	1000	50	1900–2150	2010.1
France (Site 2)	1000	1000	50	1900–2150	2010.1
France (Site 3)	1000	1000	50	1900–2150	2010.1
Israel	1000	1000	50	1750–2000	1882.5
The Netherlands	1000	1000	50	1950–2200	2073.0
USA	200	200	60	2150–2400	2279.7

ure-of-eight antenna was used in order to improve the signal-to-noise ratio before filtering.

A first appraisal of noise can be made by computing its RMS amplitude as

$$\eta = \frac{1}{N}\sum_{i=1}^{N}\sqrt{X_i^2 + Y_i^2}, \tag{9}$$

where N is the number of samples in a noise record after the synchronous detector. An example of noise measurements in France is shown in Fig. 2. At each site, 40 consecutive 1000-ms long records of the noise were made, at about 10-s intervals. The sampling rate was 2 ms which makes $N=500$ in Eq. (9). It can be seen that even at the same test site, the noise magnitude was not stable and may vary by a factor of more than 2.

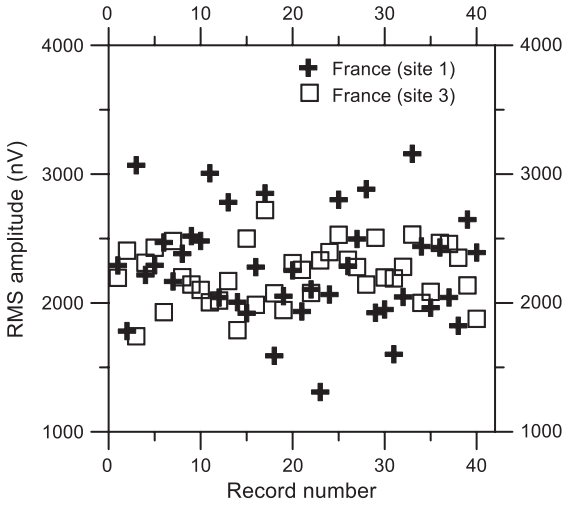

Fig. 2. Variations in the magnitude of power-line noise.

A more detailed analysis was made using the Fourier transform. Fig. 3 shows the Fourier spectra of noise records at four different test sites. Industrial frequency harmonics dominate in all the spectra. However, the amplitudes of even and odd harmonics and the nonharmonic noise vary significantly from one site to another. Note that, as the records from the USA are for relatively short time periods (200 ms instead of 1000 ms), the bandwidth of power-line harmonics in the USA spectrum appears correspondingly wider.

Industrial frequency stability is the keystone of the power-line noise filtering techniques proposed by Butler and Russell (1993). In 1993 and later (Butler, 2001), the authors showed the consequences of incorrect frequency estimation on the performance of subtraction schemes. In order to check the stability assumption, measurements were made of power-line harmonic frequencies in the investigated frequency range (37th harmonic in Israel, 40th in France and 41st in the Netherlands) using the synchronous detector described above. It can be seen (Fig. 4) that frequencies vary from one record to another but the instability is site-dependent with the largest variations being observed in Israel. Such considerable instability of an industrial frequency is, in fact, very unusual and there is no clear reason why it occurs. However, even in the same country (France, Sites 1 and 2), the frequency estimates show some instability. This instability (variations around 0.5 Hz and even higher) can be explained partly by instability of the power-line fundamental frequency, and partly by noise influencing the accuracy of the estimation.

The proportion of 50-Hz harmonics in the noise spectra was also calculated (Fig. 5). In order to diminish the spectral leakage effect caused by limited resolution of the Fourier transform on the accuracy of

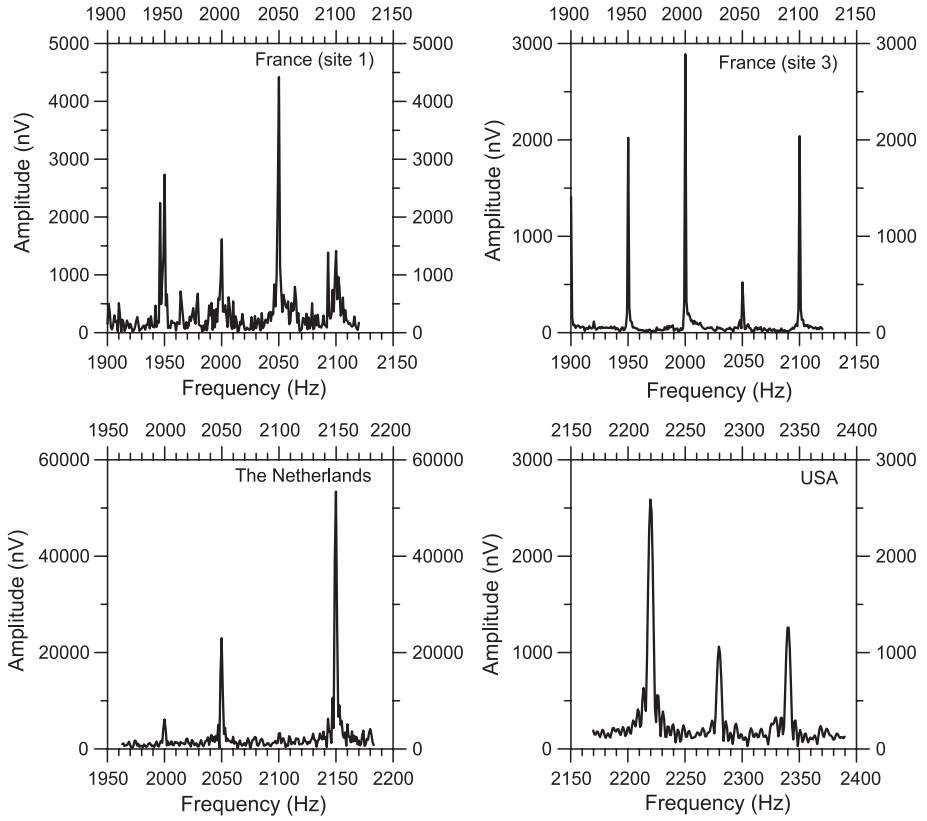

Fig. 3. Examples of power-line spectra.

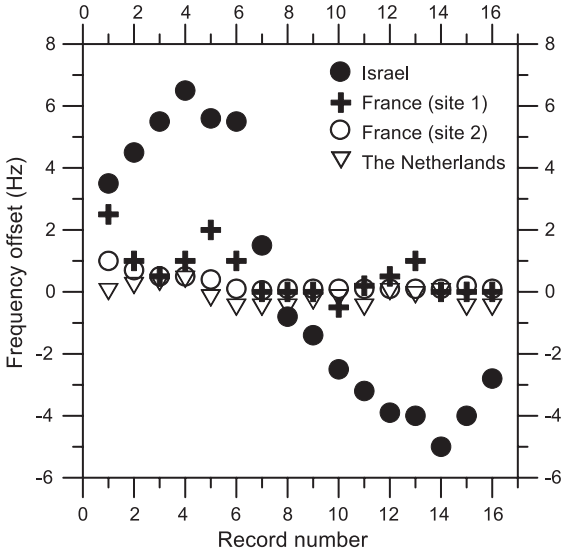

Fig. 4. Frequency of power-line harmonics.

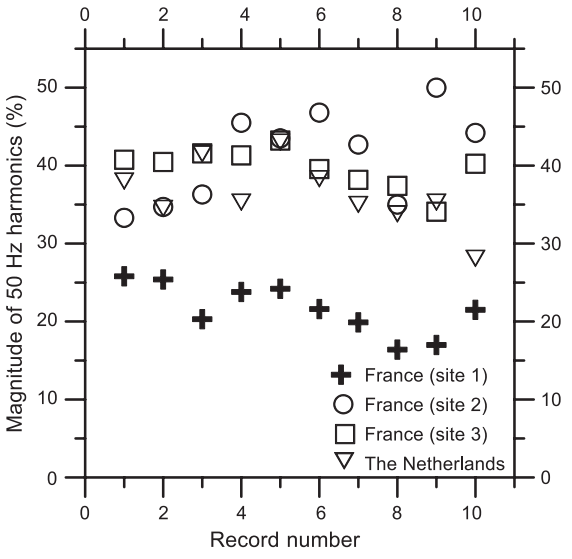

Fig. 5. Proportion of 50-Hz harmonics in the total noise.

the estimation, the ±1 Hz bandwidth around each harmonic was taken into account for the calculations. It was found that, depending on the site, the power-line harmonics represent only 20–50% of the noise energy within the ±150 Hz bandwidth centred at about 2000 Hz (Table 1). This high percentage of nonstationary noise observed in the vicinity of power lines may be explained by the fact that in the investigated frequency range the most energetic (and probably more stable) lower harmonics are filtered out and only the higher harmonic numbers (20–55) are used. It is also possible that power lines, being long conductors, act as electromagnetic antennae and channel both man-made and natural electromagnetic noises from a large area, thus amplifying the grossly random background noise, especially on the vertical magnetic component that is measured with MRS antennae.

4. Block subtraction

After the synchronous detector and low-pass filter, only three power-line harmonics around the Larmor frequency can be considered harmful for MRS signal measurement: $f_{k-1}=\Delta F-50$, $f_k=\Delta F$, and $f_{k+1}=\Delta F+50$, where $\Delta F=(50k-f_{sd})$, $f_{sd}\approx f_0$ and k is closest to the Larmor frequency power-line harmonic.

For practical implementation of the block subtraction method, it is assumed that the noise is regular and largely dominant over the signal (otherwise, filtering would not be needed) and, therefore, that nonstacked signal records are mostly noise. The block subtraction method for such a case is shown in Fig. 6. The strategy consists of selecting the time shift τ so that the noise sample $B(t)$ from a noise record, and the sample $A(t)$ that contains both signal and noise, are as similar as possible. An ideal sample rate would be an integer multiple of 50 Hz. However, the finite sample interval of the record and uncertainty over the exact value of the fundamental frequency limits the accuracy of the subtraction in this case. In order to diminish errors caused by erroneous estimation of the fundamental frequency, the correlation function between a fixed sample $A(t)$ and a moving sample $B(t)$ are used as criteria for the best selection of τ:

$$R_{AB}(t,\tau)=\left[\frac{\int_{t_4}^{t_5}X_A(t)X_B(t-\tau)\mathrm{d}t}{\sqrt{\int_{t_4}^{t_5}X_A^2(t)\mathrm{d}t\int_{t_1}^{t_2}X_B^2(t)\mathrm{d}t}}+\frac{\int_{t_4}^{t_5}Y_A(t)Y_B(t-\tau)\mathrm{d}t}{\sqrt{\int_{t_4}^{t_5}Y_A^2(t)\mathrm{d}t\int_{t_1}^{t_2}Y_B^2(t)\mathrm{d}t}}\right]\rightarrow\max, \tag{10}$$

where X and Y are the channels of the synchronous detector and $\Delta t=t_2-t_1=t_5-t_4$ ($\Delta t=200$ ms for a typical NUMIS setup).

An ideal noise sample would be when $R_{AB}(t,\tau)=2$, but in practise the best value τ_{best} is when

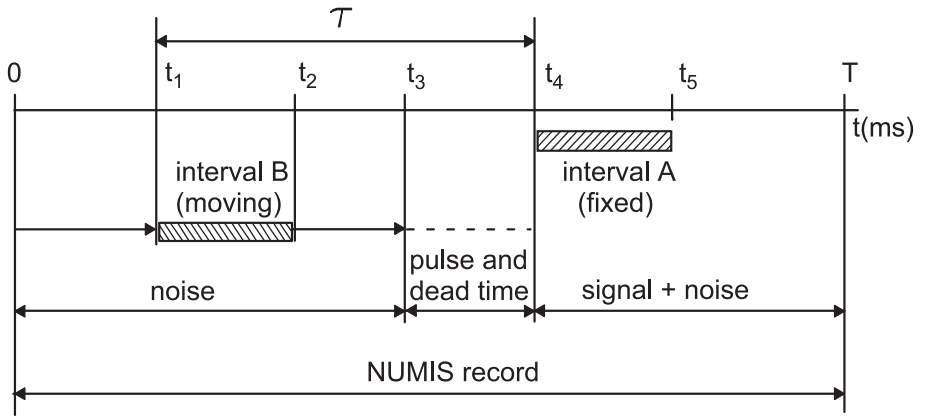

Fig. 6. Selection of the best noise block from a noise record.

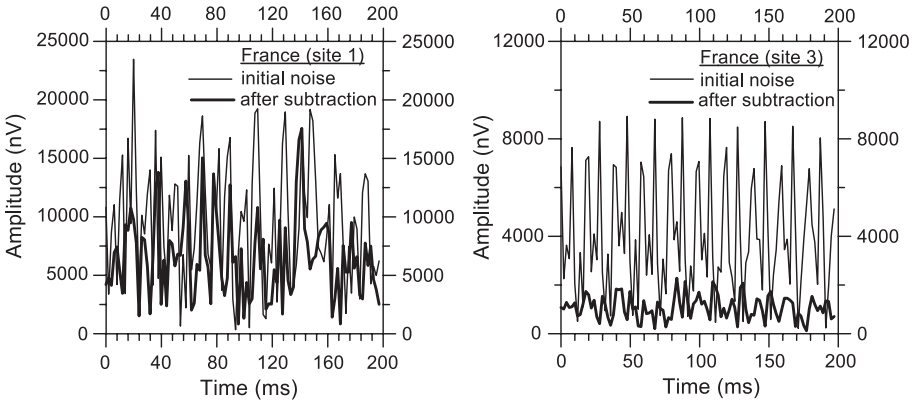

Fig. 7. Examples of the block subtraction application.

$R_{AB}(t,\tau_{best}) = \max$. The efficiency of block subtraction can be demonstrated using two different noise records made in France. In Fig. 7, the amplitude of noise sample ($A(t)$), after processing by the synchronous detector $(A(t)) = \sqrt{X^2(t) + Y^2(t)}$, is plotted versus time and shown by the thin line. The mean value of the amplitude is given by the 2000-Hz harmonic, but the 1950-Hz and 2050-Hz harmonics are also clearly seen on the plot. As $\Delta F = -10$ Hz for these sites (Table 1), the harmonics are presented as a combination of 40- and 60-Hz sinusoids, respectively. The results of the subtraction $(A(t) - B(t))$ is depicted by the thick line. For the record from Site 1, $R_{AB}(t,\tau_{best}) = 1.4$ and the subtraction is inefficient, whereas for Site 3, $R_{AB}(t,\tau_{best}) = 1.92$ and the subtraction technique works well. If the proportion of 50-Hz harmonic in the power-line noise recorded at Site 1 (about 20%) is compared with Site 3 (about 40%) (Fig. 5), it can be concluded that the block subtraction method gives better results when the percentage of 50-Hz harmonics (regular part) is larger. This conclusion matches exactly that of Butler and Russell (1993) concerning the efficiency of the block subtraction technique for the 0.1–1000 Hz frequency range.

5. Sinusoid subtraction

The sinusoid subtraction technique is based on the representation of power-line noise as harmonics superimposed on the fundamental frequency (50 or 60 Hz). The harmonic component is estimated from noise records and then subtracted from records containing both the signal and noise. The frequency of power-line harmonics, being relatively unstable, should not be determined by simply multiplying the fundamental frequency value by an integer number. During fieldwork, estimates must be made from the records, not only of the amplitude and phase of a power-line harmonics but also its frequency.

When applying this technique to MRS signal filtering, it should be kept in mind that the harmonics furthest from the Larmor frequency f_0 are filtered out by the low-pass filter and do not influence MRS measurement accuracy. The few interfering harmonics (usually three, but sometimes five) are close to f_0. In the NUMIS system, synchronous detectors (three or five) are used for power-line harmonics estimation (amplitude, phase and frequency), in a manner very similar to that applied to signal processing (Section 2.2). For each synchronous detector, the reference frequency is set equal to one of the few fundamental harmonics frequencies close to the Larmor frequency: $f^k_{sd} = 50k$. The low-pass filter has a bandwidth of 5 Hz instead of 100 Hz. If the fundamental frequency is sufficiently stable, or varies slowly and thus can be considered stable during a few seconds period, the harmonics can be estimated using a noise record before the pulse ($e_0 = 0$ in Eqs. (4) and (5)). Otherwise, a record after the pulse can be used on the assumption that the noise is much larger than the signal ($p_k >> e_0$ for all $k \in K$, in Eqs. (4) and (5)). Obviously, there is no need to compute the logarithm for the harmonics amplitude estimation (Eq. (6)).

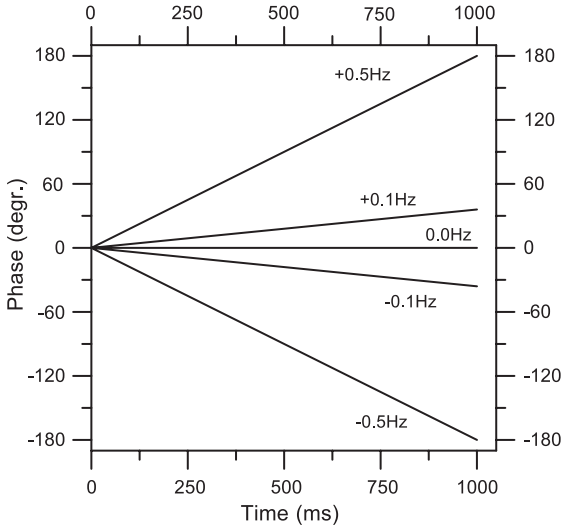

Fig. 8. Phase shift caused by different frequency offsets δf.

Modeling results show that, using a 1-s record, the power-line harmonic frequency can be measured reliably to within an error of ± 0.1 Hz. For example, assuming that for kth harmonic $p_k >> (e_0 + \varepsilon(t))$ and $\varphi_k = 0$, phase $\Phi(t) = 2\pi\delta f_k t$ is calculated after the synchronous detector (Eq. (7)) by varying $\delta f_k = (f_{sd} - f_k)$ as shown in Fig. 8. This example demonstrates that margins of error even smaller than 0.1-Hz error can easily be achieved but, in practise, nonregular noise may corrupt the phase measurements $\Phi(t)$ and diminish the accuracy.

6. Notch filtering

When designing a low-pass filter for the MRS system, it should be kept in mind that the relaxation time of the magnetic resonance signal T_2^* varies typically from 40 to 400 ms and this determines the bandwidth of the filter. The Larmor frequency cannot be considered as constant because it is affected by geomagnetic field variations within the volume investigated by MRS and also is unstable over time, and hence the bandwidth of the filter must be increased to about 4 Hz. The notch filter is centred on the power-line harmonic frequencies; as these are known only approximately, the filter cuts out ± 1 Hz bandwidth around each harmonic. A combined filter, consisting of a low-pass filter centred on the Larmor frequency and a ± 1 Hz notch filter centred as close as possible to the harmonic of the fundamental frequency, is depicted in Fig. 9 (dashed line). It should be noted that the notch filter removes between three and five harmonics but they are not shown in Fig. 9.

Whilst the sinusoid subtraction method subtracts the estimates of power-line harmonics without distorting or attenuating the signal of interest, the notch filter always cuts out a narrow frequency band and, therefore, the signal may be deformed. It is thus necessary to investigate the distortion effect of such a notch filter on the magnetic resonance signal.

6.1. Exponentially decaying signal

Interpretation of MRS measurements is based on amplitude inversion and relaxation time of the magnetic resonance signal. Thus, it is necessary to first investigate how notch filtering will affect an exponentially decaying signal, ignoring for the moment the frequency offset and phase shift that occur in real signals.

Filtered signals of 100 nV initial amplitude (e_0), 100 ms relaxation time constant (T_2^*), with no frequency shift between the Larmor frequency and the

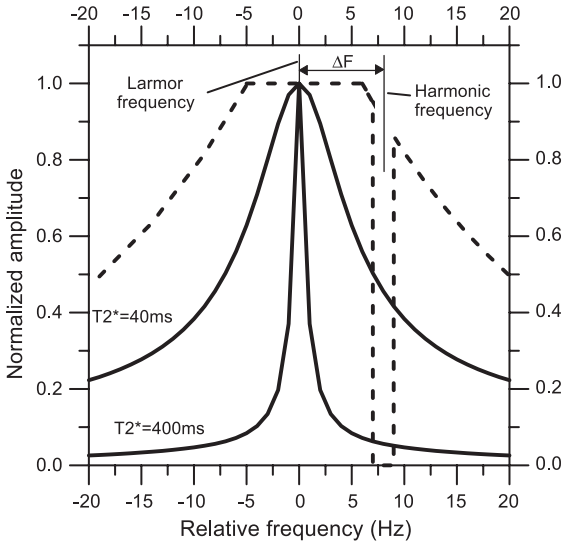

Fig. 9. Spectra of the exponential signal (solid lines) and combined low-pass and notch filter (dashed line).

reference frequency of the synchronous detector ($\delta f = f_{sd} - f_0 = 0$), and zero phase ($\varphi_0$), are plotted in Fig. 10. A 50-Hz power-line frequency is assumed. The six cases (Fig. 10) correspond to various values of the difference between the Larmor frequency and the closest power-line harmonic $\Delta F = (f_k - f_{sd})$, where $f_k = 50k$. In each case, f_{k-1}, f_k and f_{k+1} are set to 0 in the Fourier spectrum. When $\Delta F \neq 0$, the filtering cancels cosine and sine components, thus inducing oscillations, and when $\Delta F = 0$, a downward shift is also induced. These various effects create some bias when estimating the parameters of the filtered signals which is decreasing when $\Delta F \geq 4$ Hz. The worst case is when $\Delta F = 0$, since the signal is corrupted by the downward shift of the curve and consequently the time constant is strongly underestimated.

The question then arises, as to whether application of the notch filter provides better practical results, or whether its application causes more inaccuracies to the signal than the power-line noise.

In order to tackle this question, work was carried out on purely synthetic examples; the results of 100 different noise determinations were averaged and used to derive the requisite statistics. Firstly, a set of 100 synthetic signals was produced using a random number generator. Secondly, values were set of $\delta f = 0$ and

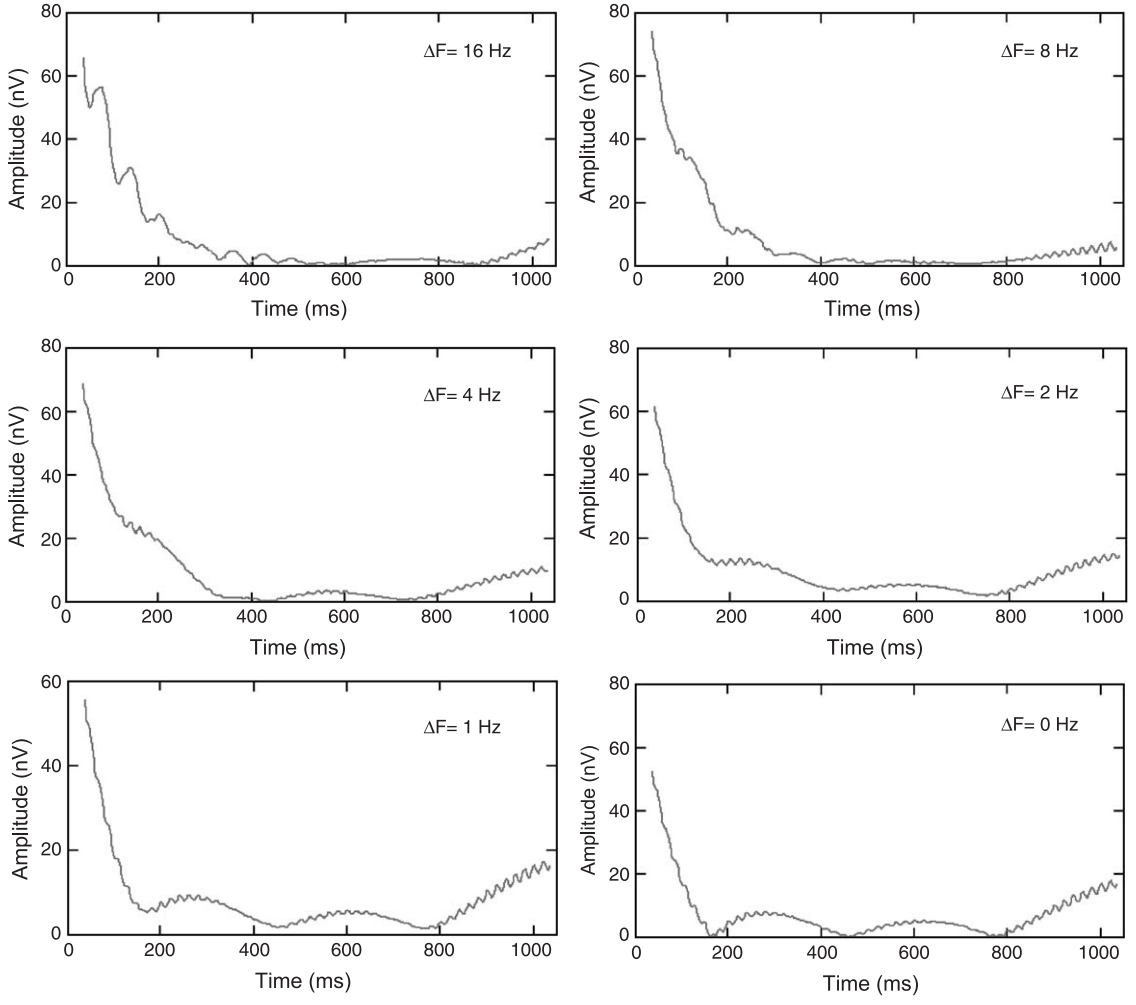

Fig. 10. Examples of the exponential signal ($T_2^* = 100$ ms) distorted by notch filtering for various values of the frequency offset ΔF.

$\varphi_0 = 0$ and thus, after the synchronous detector (Eqs. (4) and (5)), $Y(t) = 0$ and

$$X(t) = e_0 \left(e^{-t/T_2^*} + \alpha e^{-2\pi i t \Delta F - \mathrm{random}_{-\pi}^{+\pi}} + \beta \frac{\mathrm{random}_{-1}^{+1}(t) + i \cdot \mathrm{random}_{-1}^{+1}(t)}{\sqrt{2}} \right), \quad (11)$$

where α and β are the relative power-line harmonic and the relative white noise magnitudes. The time series was 1000 ms long (with 2 ms sampling). The amplitude e_0 and time constant T_2^* were taken as 100 nV and 100 ms, and the relative noise coefficients α and β as 0.4 and 0.2, respectively. Five values of the frequency offset (ΔF) were used for the power-line noise simulation: 1, 2, 4, 8 and 16 Hz. Each synthetic record was first smoothed by the low-pass filter discussed above (Fig. 9), with and without notch filtering. The signal parameters (e_0 and T_2^*) were estimated using the fitting algorithm presented in Section 2.2, which are sets $\delta f = 0$ and $\varphi_0 = 0$. The average and standard deviation of the obtained parameters for all 100 estimates were then calculated for the relevant parameters (Table 2).

Modeling results show that application of the notch filter significantly improves accuracy of signal parameter estimation for all the power-line frequency offset values. The notch filter efficiently eliminates the sinusoidal noise and there is practically no distortion to the synthetic signal when $\Delta F > 4$ Hz. For smaller values of the frequency offset ($\Delta F \leq 4$ Hz), the notch filter corrupts the signal. However, the noise influence on unfiltered signals is even more harmful and quite often leads to fitting instability, as shown by much lower stable fitting occurrence percentages, and sometimes to unrealistic parameters (ERR in Table 2).

6.2. Complete magnetic resonance signal

Section 6.1 considered a simplified magnetic resonance signal, neglecting the frequency offset (δf) and phase shift (φ_0). Notch filtering was shown to be an efficient approach, and Section 6.2 is concerned with the performance of the filtering technique when applied to complete magnetic resonance signals.

The first step was to compare a ± 1 Hz notch filter with a single-harmonic notch filter, the latter being a compromise between a notch filter and sinusoid subtraction. Sinusoid subtraction requires accurate determination of the amplitude, frequency and phase of the harmonics, whereas only the frequency is important for the single-harmonic notch filter.

For modeling, a synthetic signal with fixed parameters ($e_0 = 100$ nV; $\delta f = 0$ Hz; $\varphi_0 = 0°$) was used and the relaxation time was varied; T_2^* (100, 200 and 400 ms). The time series of 1000 ms each (X and Y) were computed using Eqs. (4) and (5), assuming $p(t) = 0$ and $\varepsilon(t) = 0$. The model was set to $\delta f = 0$ and $\varphi_0 = 0$, so initially $Y(t) = 0$, but after notch filtering the signal is deformed, which creates a nonzero $Y(t)$ component. A nonlinear fitting algorithm (Section 2.2) was used to estimate signal parameters with a relative error of

$$\mathrm{err} = \frac{P_{\mathrm{est}} - P_{\mathrm{true}}}{P_{\mathrm{ref}}} 100\%, \quad (12)$$

where P_{est} is the estimate of a parameter, P_{true} is the true value of this parameter used in the model, and P_{ref} is the reference value for computing the relative error. The optimisation method for nonlinear fitting operates within the 16-Hz frequency range, so this value was used as the reference; $P_{\mathrm{ref}} = 16$ Hz. For the phase $P_{\mathrm{ref}} = 360°$, and for the amplitude and the relaxation time $P_{\mathrm{ref}} = P_{\mathrm{true}}$.

Table 2
Results of statistical analysis of the influence of power-line harmonics notch filtering on the estimates obtained for e_0 and T_2^*

ΔF		1 Hz		2 Hz		4 Hz		8 Hz		16 Hz	
Notch filter		No	Yes	No	Yes	No	Yes	No	Yes	No	Yes
Stability of fitting scheme		0%	100%	7%	100%	29%	100%	100%	100%	100%	100%
e_0 (nV)	average	err	90	54	71	95	83	149	94	108	97
	stand. deviation	err	± 11	N/A	± 5	± 100	± 4	± 69	± 4	± 26	± 5
T_2^* (ms)	average	err	70	354	109	251	113	86	104	98	102
	stand. deviation	err	± 9	err	± 10	± 416	± 6	± 33	± 4	± 18	± 5

Modeling results (Fig. 11) show the relative errors versus the frequency offset ΔF. As expected, the single-harmonic notch filter induces smaller errors than the ± 1 Hz notch filtering, and thus can be used in the frequency range $|\Delta F|>1$ Hz. The ± 1 Hz notch filter can be considered harmless when $|\Delta F|>8$ Hz for all the signals. For short signals ($T_2^*<100$ ms), this interval could be extended to $|\Delta F|>4$ Hz. In the vicinity of harmonic frequency ($|\Delta F|<4$ Hz), the signal is too corrupted by the filtering and the results are unreliable.

6.3. Signal distortion compensation

When $|\Delta F|<8$ Hz, the ± 1 Hz notch filter deforms the signal, causing inaccuracies in parameter estimates. However, such filtering errors can be partly corrected if there is compensation for distortion in the fitting algorithm, as described below.

If ψ is the notch filtering operator, then $\psi[X(t)]=\tilde{X}(t)$ and $\psi[Y(t)]=\tilde{Y}(t)$ are the filtered records. To compensate for filter distortion, the curve fitting nonlinear regression method (Section 2.2) in Eq. (8) should be modified as follows:

$$\left[\int_{\Delta t}\left(\tilde{X}(t)-\psi[X_{\mathrm{mod}}(t)]\right)^2 \mathrm{d}t+\int_{\Delta t}\left(\tilde{Y}(t)-\psi[Y_{\mathrm{mod}}(t)]\right)^2 \mathrm{d}t\right]\rightarrow \min, \tag{13}$$

where Δt is the record length.

When $\Delta F\rightarrow 0$, the frequency and phase information may be irretrievably lost even when using Eq.

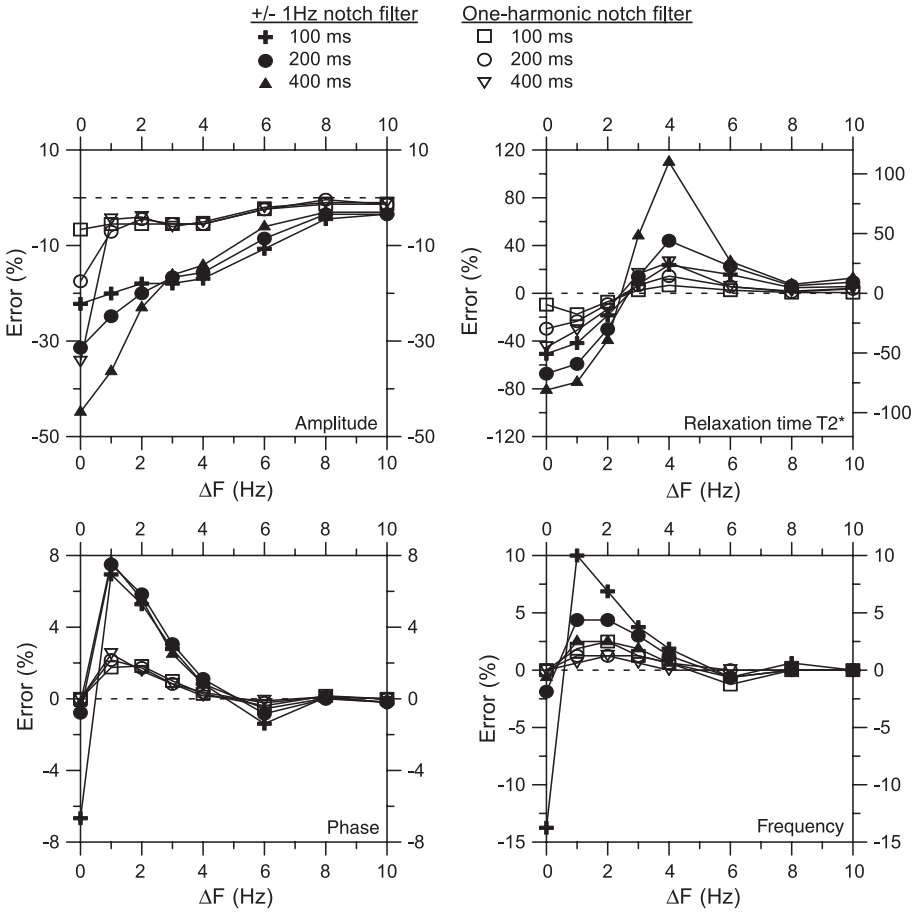

Fig. 11. Errors in signal parameter estimation caused by notch filtering for various values of the frequency offset ΔF.

(13). In this case, only the amplitude e_0 and the relaxation time T_2^* can be estimated, and Eq. (8) in the fitting scheme should be replaced by:

$$\left[\int_{\Delta t}\left(\sqrt{\tilde{X}^2(t)+\tilde{Y}^2(t)}-\psi[E_{\mathrm{mod}}(t)]\right)^2 \mathrm{d}t\right]\rightarrow \min, \tag{14}$$

where $E_{\mathrm{mod}}(t)=e_0\exp(-t/T_2^*)$.

The criteria for deciding whether Eqs. (13) or (14) should be used is the accuracy of the Larmor frequency estimate. Let f_0^e be the signal frequency estimate (the Larmor frequency in the subsurface) obtained by minimisation of Eq. (13). The Larmor frequency estimate on the surface (f_0^s) is always determined from measurements of the geomagnetic field. Thus, if $|f_0^e-f_0^s|<1$ Hz, then Eq. (13) can be used; otherwise, it must be replaced by Eq. (14).

The efficiency of the distortion compensation approach can be demonstrated using records from Section 6.2. Amplitude and relaxation time estimation errors caused by the ± 1 Hz notch filtering were corrected by applying the distortion compensation, and modeling results (Fig. 12) showed significant improvements in accuracy. When $|\Delta F|>4$ Hz, any errors were completely compensated. For signals with $T_2^*<100$ ms, the distortion correction enabled correct amplitude determination even when the Larmor frequency coincided exactly with a power-line harmonic. For signals with $T_2^*>100$ ms, however, the improvement was smaller because the filter cut out a large part of the signal energy.

6.4. Synthetic signal with real noise

The next step was to ascertain the critical value of the signal-to-noise ratio (S/N) above which the signal parameters can be reliably estimated.

The same model was used as in previous sections ($e_0=100$ nV; $T_2^*=100$ ms; $\delta f=0$ Hz; $\varphi_0=0°$). The time series ($X_{(\mathrm{mod})}(t)$ and $Y_{(\mathrm{mod})}(t)$) were computed using Eqs. (4) and (5), assuming $p(t)=0$ and $\varepsilon(t)=0$. Real noise records ($X_{(\mathrm{noise})}(t)$ and $Y_{(\mathrm{noise})}(t)$) made at three test sites (two in France, one in the Netherlands) were added to the synthetic signal, and 40 different noise records from each site were used. For varying S/N, the noise was attenuated before adding it to the signal; $E(t)=E_{(\mathrm{mod})}(t)+aE_{(\mathrm{noise})}(t)$. The record length was 1000 ms and the sampling rate was 2 ms for both signal and noise. Whilst the full record length (1000 ms) was used for filtering, only the first 200 ms was used for signal parameter estimation. The signal-to-noise ratio was thus calculated for the first 200 ms (100 samples);

$$\mathrm{S/N}=\sum_{i=1}^{100}\sqrt{X_{(\mathrm{mod})i}^2+Y_{(\mathrm{mod})i}^2}\Bigg/\left(a\sum_{i}^{100}\sqrt{X_{(\mathrm{noise})i}^2+Y_{(\mathrm{noise})i}^2}\right). \tag{15}$$

The signal parameters were estimated from these noise-corrupted records both with and without application of the ± 1 Hz notch filter, and then the relative

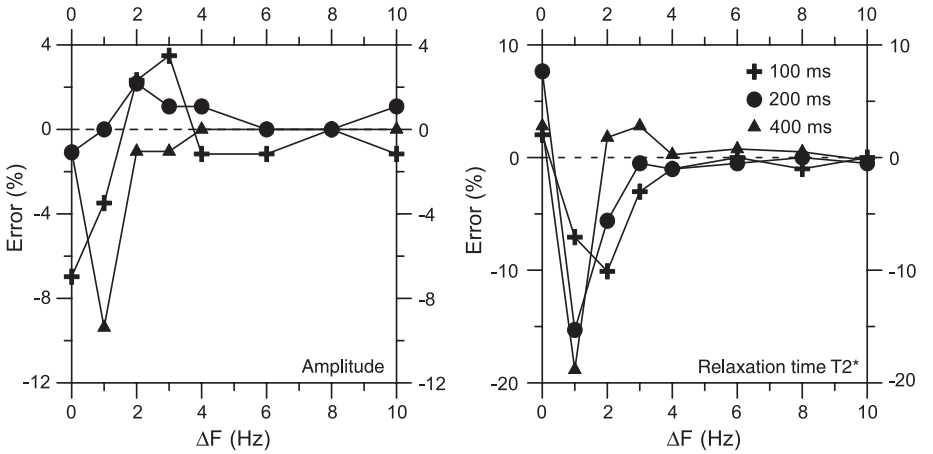

Fig. 12. Demonstration of the efficiency of distortion compensation.

Table 3
Threshold of reliable estimation of the MRS signal parameters

Test site	Critical S/N notch OFF	Critical S/N notch ON	Improvement in S/N
The Netherlands	0.16	0.07	2.28
France (Site 1)	0.8	0.08	10
France (Site 2)	0.1	0.01	10

error of each parameter estimation was calculated using Eq. (12). For each signal parameter, the average relative error and standard deviation were calculated, respectively, as;

$$\mu = \frac{1}{40}\sum_{m=1}^{40} \mathrm{err}_m, \tag{16}$$

and

$$\sigma = \frac{1}{40}\sum_{m=1}^{40} \sqrt{(\mathrm{err}_m - \mu)^2}. \tag{17}$$

Values μ and σ were analysed for different S/N ratios for each separate test site. The improvement in signal parameter estimation due to the filtering algorithm can be evaluated by considering the S/N for which the nonlinear fitting algorithm becomes unstable as the critical value. The results are summarised in Table 3. Depending on the test site, the critical value of S/N varies between 0.8 and 0.1 without the notch filter and between 0.01 and 0.08 with the notch filter. The improvement in the critical S/N is between 2.3 and 10 times depending on the site.

7. Efficiency of power-line noise reduction

The efficiency of the filtering techniques was estimated using 40 consecutive noise records made at each of four test sites (France, three; Netherlands, one). As previously, record length was 1000 ms with 2-ms sampling rate and noise reduction estimation for only the first 200 ms.

For each site, if $m = 1,2,\ldots,40$ is the number of a record; $i = 1,2,\ldots,100$ is the number of a sample within each record; and $X_{(m)i}$ and $Y_{(m)i}$ are noise samples, then within one record the noise RMS amplitude is

$$\eta_m = \frac{1}{100}\sum_{i=1}^{100} \sqrt{X_{(m)i}^2 + Y_{(m)i}^2}, \tag{18}$$

the noise mean value over 40 records is

$$\mu = \frac{1}{40}\sum_{m=1}^{40} \eta_m, \tag{19}$$

and its standard deviation is

$$\sigma = \frac{1}{40}\sum_{m=1}^{40} \sqrt{(\eta_m - \mu)^2}. \tag{20}$$

Estimating the noise RMS amplitude for unfiltered records (raw data) and applying different filtering methods (block subtraction, sinusoid subtraction and $\pm$ 1 Hz notch filtering), the noise reduction factors can be calculated by:

$$k_\mu^{\mathrm{scheme}} = \mu^{\mathrm{raw}}/\mu^{\mathrm{scheme}}, \tag{21}$$

and

$$k_\sigma^{\mathrm{scheme}} = \sigma^{\mathrm{raw}}/\sigma^{\mathrm{scheme}}, \tag{22}$$

where "scheme" superscript indicates which method was applied.

The results shown in Table 4 indicate that the efficiency of the noise filtering methods depends on

Table 4
Efficiency of the noise reduction at different sites

		France (Site 1)	France (Site 2)	France (Site 3)	The Netherlands
noise amplitude	μ^{raw}	2269	31,485	2222	18,544
	μ^{notch}	1350	5653	390.5	9721
	μ^{sinusoid}	1597	7016	547	10,623
	μ^{block}	1830	5901	466	7540
noise standard deviation	σ^{raw}	329	1397	183.9	1990
	σ^{notch}	246	878	52	1226
	$\sigma^{\mathrm{sinusoid}}$	272	1134	80	1168
	σ^{block}	303	1375	88	1484
noise reduction factor	k_μ^{notch}	1.7	5.6	5.7	1.9
	$k_\mu^{\mathrm{sinusoid}}$	1.4	4.5	4.1	1.7
	$k_\sigma^{\mathrm{block}}$	1.2	5.3	4.8	2.5
	$k_\sigma^{\mathrm{notch}}$	1.3	1.6	3.5	1.6
	$k_\sigma^{\mathrm{sinusoid}}$	1.2	1.2	2.3	1.7
	$k_\sigma^{\mathrm{block}}$	1.1	1.0	2.1	1.3

Table 5
Optimal selection of the filtering technique

Filter	T_2^*= 100 ms	T_2^*= 200 ms	T_2^*= 400 ms
± 1 Hz notch filter	ΔF>4 Hz	ΔF>6 Hz	ΔF>8 Hz
Sinusoid subtraction	ΔF<4 Hz	1<ΔF<6 Hz	2<ΔF<8 Hz
Block subtraction	ΔF<1 Hz	ΔF<1 Hz	ΔF<2 Hz

the test site. The best results are obtained at Sites 2 and 3 (France) where the noise contains the largest percentage of 50-Hz harmonics (Fig. 5). At the same site, notch filtering appears to be the most efficient for noise reduction as it cuts out the largest bandwidth. The sinusoid subtraction and the block subtraction are, respectively, less efficient. However, it should be remembered that when the Larmor frequency is close to one of the power-line harmonic frequencies, the notch filtering might also distort the signal of interest. So, depending on the noise and the frequency offset, a compromise must be made between removing the noise and keeping the signal undisturbed so that signal parameters can be estimated.

Basing on experience gained to date, the rule for filtering method selection is proposed (Table 5). It can be shortly summarized as following:

- When the frequency offset $|\Delta F|$>8 Hz, the notch filter is the most effective.
- When $|\Delta F| < 8$ Hz, the notch filter may be too drastic and suppress important signal information for long relaxation times (T_2^*>200 ms) and, in this case, the subtraction techniques must be used.

8. Example of application

The results obtained in France with NUMIS instrumentation using a 75-m-side square loop can be used to demonstrate the method. Noise magnitude was found to be about 900 nV (16×10^{-11} T approximately) and, for this level of a noise, a stacking procedure was necessary to improve the signal-to-noise ratio. Spectral analysis revealed a high percentage of 50-Hz harmonics, which suggested that one of the power-line filtering techniques may be suitable. The Larmor frequency, measured with a proton magnetometer, was 2010 Hz. As $|\Delta F|$>8 Hz, the ± 1 Hz notch filtering scheme without the distortion compensation could be applied and records were filtered before stacking ($X(t) = \frac{1}{N}\sum_{i=1}^{N} \psi[X_i(t)]$ and $Y(t) = \frac{1}{N}\sum_{i=1}^{N} \psi[Y_i(t)]$ with N being the stacking number). Two soundings were performed at the same site: (a) with 200 stacks without notch filtering; (b) with 10 stacks that were processed with and without notch filtering. It was considered that sounding (a) provided true data and it was therefore compared with two other soundings.

Fig. 13 shows NUMIS records (after the synchronous detector) made with the same value of the pulse parameter containing both the signal and the noise: (1) one stack after only hardware filtering; (2) same as (1) but with the low-pass filter (Fig. 9) without notch filtering; (3) after 200 stacks and the low-pass filter,

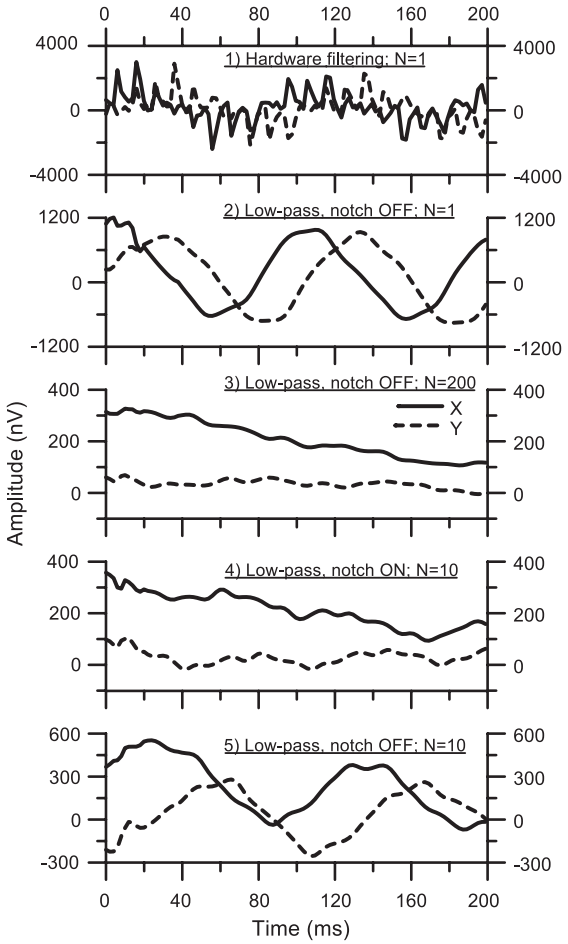

Fig. 13. Field example; filtering of signal records.

without notch filtering; (4) after 10 stacks and the low-pass filter, with notch filtering; (5) same as (4) without notch filtering. It can be seen that application of notch filtering allows signal recovery using 10 stacks with about the same degree of accuracy as using 200 stacks without notch filtering.

Signal parameters estimated for these three soundings against the pulse parameter are shown in Fig. 14. It is clear that the results obtained using 10 stacks and applying the notch filtering are close to those made with 200 stacks. As the signal frequency estimate corresponds well to the proton magnetometer measurements (2010 Hz) and the phase varies smoothly, it can be concluded that the magnetic resonance signal was detected reliably. Using 10 stacks without the notch filtering, the signal frequency estimate is about 2000 Hz which corresponds to the 40th harmonic of 50 Hz. Unlike the magnetic resonance signal frequency, the power-line frequency is not synchronized with the pulse and, thus, the phase derived from the records is understandably nonregular.

Comparison of MRS results with the corresponding borehole log (Fig. 15) shows that the aquifer was well detected in two cases; using the data acquired with 200 stacks, and with 10 stacks and notch filtering. Comparison between these two data sets (water content $w(z)$ and relaxation time $T_2^*(z)$) also shows reasonable agreement. Inversion of the data set with 10 stacks without notch filtering provides unrealistic results that can be easily explained as lack of accuracy due to power-line noise.

One sounding consists of the signal parameter estimation for 10–20 different values of the pulse parameter. Each value of the pulse parameter had stacking applied. For the NUMIS system, the time interval between two consecutive records is about 6 s. Thus, the time spent in the field could be estimated as $10 \times 10 \times 6 = 600$ s (plus time for the loop setup)

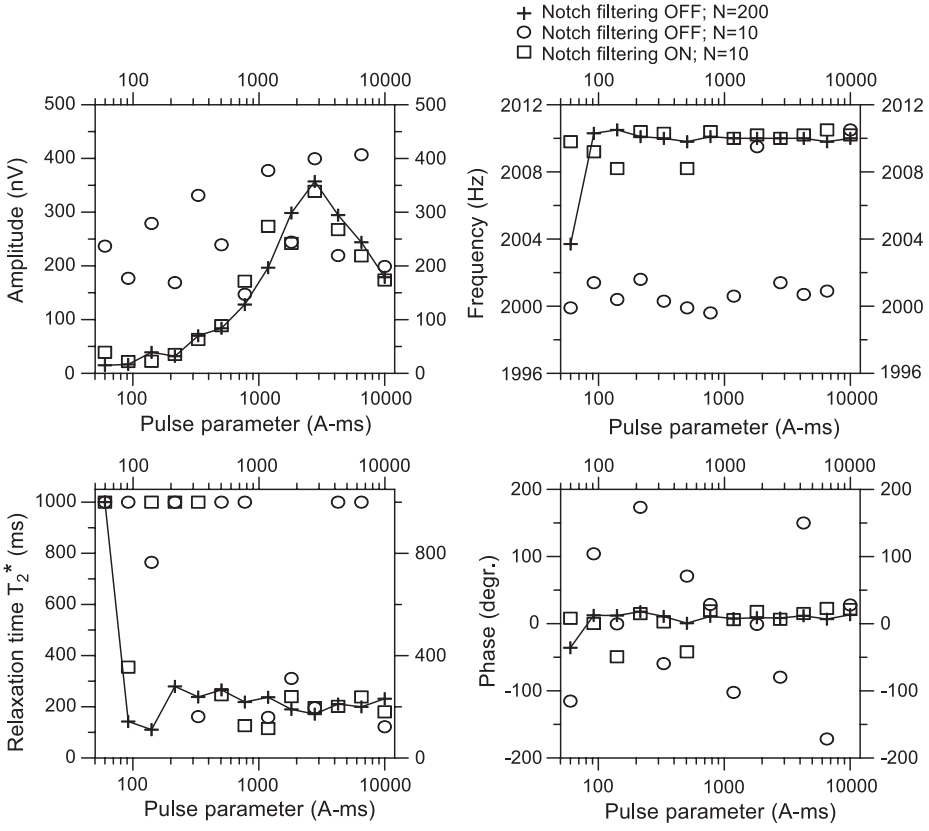

Fig. 14. Field example; MRS signal estimates when using the different filtering procedures.

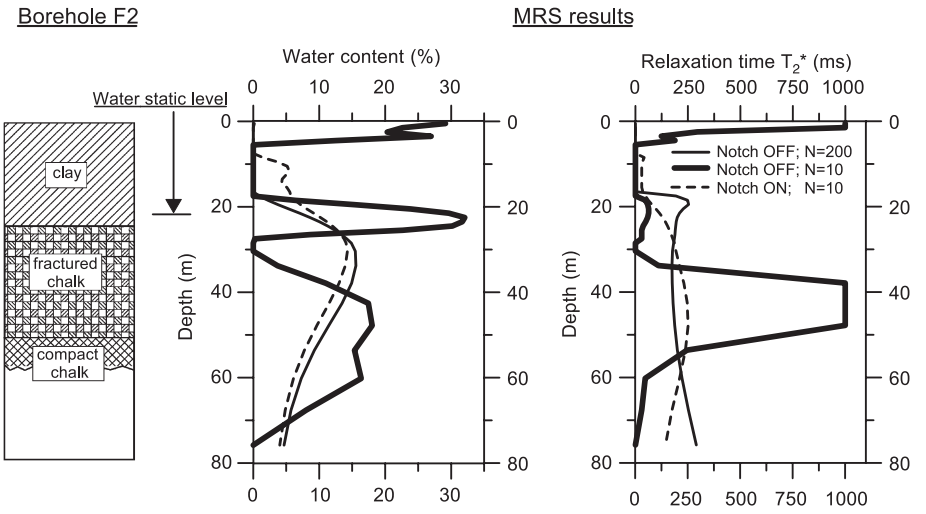

Fig. 15. Field example; borehole log and MRS inversion results when using the different filtering procedures.

when 10 stacks are used. This can be compared with the $200 \times 10 \times 6 = 12\,000$ s necessary for 200 stack soundings.

9. Conclusions

The analysis of various examples of power-line noise in the frequency range 1700–2400 Hz showed that the noise produced by electrical power lines is not completely stable and regular. The percentage of the regular component (50 Hz harmonics) may vary between 20% and 50% depending on the site. The other noise component (50–80%) is nonregular. Even for the regular component, the noise amplitude and frequency may vary within 5- to 10-s intervals.

As the percentage of 50-Hz harmonics in the power-line noise is site-dependent, the efficiency of filtering schemes based on the assumption of noise stability and regularity are also site-dependent; the more regular the noise, the more efficient is the filtering. Three existing filtering methods, block subtraction, sinusoid subtraction and notch filtering, were applied to magnetic resonance records. It was found that notch filtering was the most efficient but it distorts the signal of interest when the frequency offset between the Larmor frequency and one of the power-line harmonics is smaller than 8 Hz. In this case, the subtraction techniques are preferable. Basing on modeling results, a strategy is proposed for selecting the most appropriate filtering method by analysing the signal frequency offset and relaxation time.

Acknowledgements

The authors are grateful to Mark Goldman (Geophysical Institute of Israel), Jean Roy (ITC) and Eric White (USGS) for their participation in acquiring the field data used in this study. We also acknowledge K. Butler's comments, which helped improve the clarity of presentation.

References

Butler, K.E., 2001. Comment on "design of a hum filter for suppressing power-line noise in seismic data. Journal of Environmental and Engineering Geophysics 6 (2), 103–104.

Butler, K.E., Russell, R.D., 1993. Subtraction of powerline harmonics from geophysical records. Geophysics 58, 898–903.

Legchenko, A., Valla, P., 1998. Processing of surface proton magnetic resonance signals using non-linear fitting. Journal of Applied Geophysics 39, 77–83.

Legchenko, A., Valla, P., 2002. A review of the basic principles for proton magnetic resonance sounding measurements. Journal of Applied Geophysics 50, 3–19.

Legchenko, A., Baltassat, J.-M., Beauce, A., Bernard, J., 2002. Nuclear magnetic resonance as a geophysical tool for hydrogeologists. Journal of Applied Geophysics 50, 21–46.

Marquardt, D., 1963. An algorithm for least-squares estimation of non-linear parameters. Journal of the Society for Industrial and Applied Mathematics 11, 431–441.

Max, J., 1981. Méthodes et techniques de traitement du signal et applications aux measures physiques, tome II, troisième edition, Masson.

Schirov, M., Legchenko, A., Creer, G., 1991. New direct non-invasive ground water detection technology for Australia. Exploration Geophysics 22, 333–338.

Semenov, A.G., Schirov, M.D., Legchenko, A.V., Burshtein, A.I., Pusep, A.Yu., 1989. Device for measuring the parameter of underground mineral deposit. G.B. Patent 2198540B.

Trushkin, D.V., Shushakov, O.A., Legchenko, A.V., 1994. The potential of a noise-reducing antenna for surface NMR ground water surveys in the earth's magnetic field. Geophysical Prospecting 42, 855–862.